A mixed-valence Co_7 single-molecule magnet with C_3 symmetry†

Alan Ferguson,[a] Andrew Parkin,[a] Javier Sanchez-Benitez,[b] Konstantin Kamenev,[b] Wolfgang Wernsdorfer[c] and Mark Murrie*[a]

Received (in Cambridge, UK) 25th April 2007, Accepted 5th June 2007
First published as an Advance Article on the web 25th June 2007
DOI: 10.1039/b706238a

The synthesis, structure and magnetic properties of $[Co^{II}_4Co^{III}_3(HL)_6(NO_3)_3(H_2O)_3]^{2+}$ {H_3L = $H_2NC(CH_2OH)_3$} are reported: the complex is an exchange-biased single molecule magnet.

Single-molecule magnets (SMMs) or molecular nanomagnets are discrete molecular complexes which display slow magnetic relaxation at low temperature, due to the combination of a non-zero spin ground state and an Ising type magnetic anisotropy. Much research is being devoted to the synthesis of new examples of SMMs and the study of their magnetic properties. Different synthetic approaches have been tried by varying either the reaction conditions, such as temperature and pressure, or by using new ligands and different metal ions to those used in the prototypical Mn_{12} SMMs. One route in particular that is gaining favour is that of using anisotropic metal centres, such as lanthanide ions *e.g.* Dy(III) in combination with Mn ions[1] or transition-metal ions such as Co(II). The first complex reported to be a Co(II) SMM was a cubane and higher nuclearity cobalt(II) complexes have been shown to display slow magnetic relaxation at low temperature since then.[2,3] The cubane complex is the only Co(II) SMM that displays hysteresis loops with any significant coercivity, but these loops are complicated by strong intermolecular interactions.

We have developed a new route to mixed-valence cobalt complexes using the polydentate pro-ligand 2-[bis(2-hydroxyethyl)-amino]-2-(hydroxymethyl)propane-1,3-diol (*Bis-tris*),[4] and now extend this to the related pro-ligand 2-amino-2-(hydroxymethyl)-propane-1,3-diol [H_3L = $H_2NC(CH_2OH)_3$] as part of an ongoing project into the synthesis and study of SMMs with axial symmetry.[5] In the presence of nitrate, HL^{2-} can be used to assemble a mixed-valence Co_7 complex, which displays an interesting molecular structure with axial symmetry and beautiful crystal packing with 11 Å channels running along the *c*-axis. Bulk samples display strong, frequency dependent out-of-phase signals in the ac susceptibility below 4 K. Single crystals show temperature and sweep rate dependent hysteresis loops below 1 K, which show that the Co_7 complex is a new cobalt(II) SMM, with a very small exchange bias and hence, represents the closest example to date of an isolated Co(II) SMM showing true molecular hysteresis.

Reaction of $Co(NO_3)_2{\cdot}6H_2O$ (2.328 g, 8 mmol) with H_3L (0.969 g, 8 mmol) in H_2O (10 mL), yields a solution of pH 6.94. The pH is raised to 7.5 by addition of $NMe_4OH{\cdot}5H_2O$ (0.720 g, 3.97 mmol) and the solvent removed *in vacuo*. The residue is dissolved in MeOH (10 mL) and yields needle-like dark red crystals of $[Co^{II}_4Co^{III}_3(HL)_6(NO_3)_3(H_2O)_3][NO_3]_2{\cdot}9MeOH{\cdot}4.5H_2O$ (**1**·9MeOH·4.5H_2O) after 1 month in 5% yield.‡ Although low-yielding, the reaction is reproducible. Compound **1** crystallises in the trigonal space group, $P\bar{3}$, and contains a mixed-valence heptanuclear cobalt complex with C_3 symmetry. The central cobalt ion and three of the outer cobalt ions are ligated exclusively by oxygen donor atoms and are divalent, forming a coupled tetranuclear unit (Fig. 1). The remaining three cobalt ions, which possess a N_2O_4 ligand donor set are trivalent. Oxidation states have been assigned on the basis of bond valence sum analysis, and by consideration of bond lengths and charge balance.[6] The Co(II) and Co(III) centres have a distorted octahedral geometry. The molecule is disc-like with the cobalt centres approximately co-planar and bridged exclusively by the alkoxide groups of the di-deprotonated ligands. The HL^{2-} ligands all display the same bridging mode: one alkoxide is μ_3-bridging the central Co(II) to one outer Co(II) and one Co(III) with the second alkoxide bridging one outer Co(II) to a Co(III) centre. Each ligand amine group is

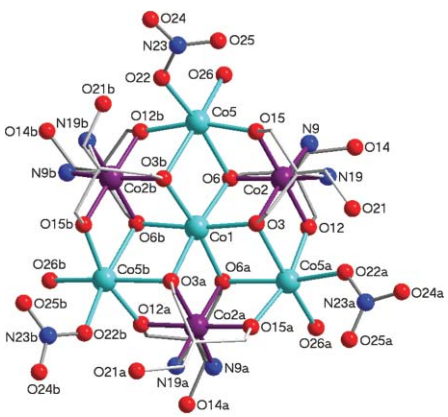

Fig. 1 Structure of the Co_7 dication {ball and stick representation with Co(II) cyan; Co(III) purple; O, red; N, blue; C, grey; H omitted for clarity}. Cobalt(II), Co(1)–O 2.09–2.10 Å; *cis* O–Co(1)–O 79.9–95.3°; *trans* O–Co(1)–O 172.9–173.0°; Co(5)–O 1.98–2.25 Å; *cis* O–Co(5)–O 75.0–106.2°; *trans* O–Co(5)–O 163.5–170.8°; cobalt(III), Co(2)–O 1.88–1.91 Å; Co(2)–N 1.91–1.92 Å; *cis* O(N)–Co(2)–O(N) 84.4–102.1°; *trans* O(N)–Co(2)–O(N) 168.9–178.4° [atom suffixes a and b signify symmetry equivalents: a = 1 − *x* + *y*, 1 − *x*, *z*; b = 1 − *y*, *x* − *y*, *z*].

[a] *WestCHEM, Department of Chemistry, University of Glasgow, University Avenue, Glasgow, UK G12 8QQ. E-mail: M.Murrie@chem.gla.ac.uk; Fax: +44 141 330 4888; Tel: +44 141 330 4486*
[b] *School of Engineering and Electronics and Centre for Science at Extreme Conditions, University of Edinburgh, West Mains Road, Edinburgh, UK EH9 3JJ*
[c] *Institut Néel, CNRS, BP 166, 25 Avenue des Martyrs, 38042, Grenoble, Cedex 9, France*

† Electronic supplementary information (ESI) available: Crystal packing diagrams showing the hydrogen bonding and further magnetisation hysteresis loops. See DOI: 10.1039/b706238a

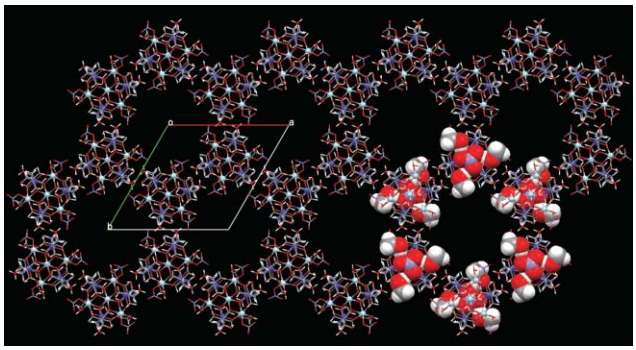

Fig. 2 Crystal packing of the Co_7 clusters, viewed along the *c*-axis (atom colour scheme as Fig. 1 plus H, white). One lattice nitrate anion and three hydrogen-bonded MeOH molecules lie above/below the Co_7 dications (highlighted bottom right in spacefill representation).

monodentate and bound to Co(III), while the final ligand CH_2OH groups are hydrogen-bonded to: for O21, a lattice MeOH molecule (O29) and an amine group (N9′) on an adjacent Co_7 molecule; for O14, a symmetry equivalent CH_2OH group on an adjacent Co_7 molecule (see ESI†). The coordination at each outer Co(II) centre is completed by a water molecule and a monodentate nitrate anion, with the nitrates found on one side of the Co_7 disc and the water molecules on the opposite side. The nitrate ligands are hydrogen-bonded to an amine group of a ligand on an adjacent Co_7 molecule (O24···N19′ 3.001 Å). Charge balance is afforded by two nitrate anions in the lattice. The crystal packing of **1** along the *c*-axis is shown in Fig. 2. One nitrate anion lies directly above the central Co(II) ion, with the N–O bonds almost coincident with the three Co(1)–O(6) bonds (torsion angle O6–Co1–N27–O28 4.38°). This leads to an interesting hydrogen-bonding motif, where this nitrate anion is hydrogen-bonded to three lattice MeOH molecules, mirroring the 3-fold symmetry of the $\{Co^{II}_4\}$ unit. The 1-D channels running along the *c*-axis have a diameter of 11 Å, and are filled with the crystallographically disordered second nitrate anion and disordered solvent (six MeOH molecules and 4.5 water molecules per Co_7).

The magnetic susceptibility of **1** is shown as χT *vs.* T in Fig. 3.‡ In a field of 1 kOe, at 300 K, χT = 9.8 cm^3 mol^{-1} K consistent with four uncoupled Co(II) ions with g = 2.28. χT rises gradually to a local maximum of 10.3 cm^3 mol^{-1} K at 100 K, before dropping to 10.0 cm^3 mol^{-1} K at 34 K. Below 34 K, χT increases more rapidly reaching a maximum of 15.6 cm^3 mol^{-1} K at 2.8 K, and finally dropping sharply to 14.8 cm^3 mol^{-1} K at 1.8 K. The characteristic strong decrease in χT often seen in Co(II) complexes as the temperature is lowered, due to a strong orbital contribution, is not seen.[7] The reason for this is two-fold: firstly, the orbital contribution is partially quenched due to the distortions from octahedral symmetry at the Co(II) centres and secondly, the increase in χT below 34 K due to the ferromagnetic exchange interactions between the Co(II) centres. Similar magnetic behaviour has been observed for a Co_{12} wheel.[8] The ferromagnetic coupling in **1** is consistent with the Co(II)–O–Co(II) bridging angles of 94°.[9] The magnetisation was measured as a function of applied field at 2 K and the data is shown in the inset of Fig. 3. At low temperature, each Co(II) can be treated as an effective spin, $S_i' = ½$ with anisotropic g values.[10] $M/N\beta$ does not reach saturation at 5 Tesla, but equals 7.65, consistent with an effective spin ground state $S' = 2$ with $g > 3.8$, arising from ferromagnetic coupling of the effective spin $S_i' = ½$ centres. This is in line with the χT data at 2.8 K, which gives $S' = 2$ and $g = 4.56$.

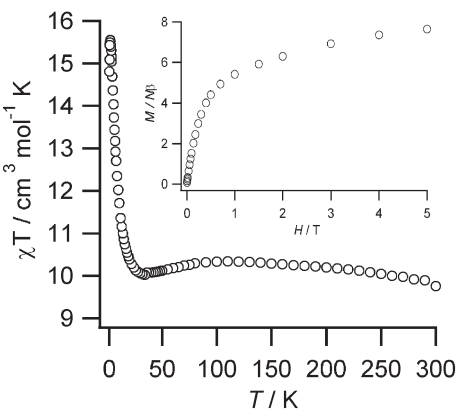

Fig. 3 Temperature dependence of χT for **1** from 300–1.8 K measured in a field of 1 kOe. Inset: magnetisation ($M/N\beta$) *vs.* H for **1** measured at 2 K.

Ac susceptibility measurements are shown in Fig. 4. The sharp decrease in χT below 2.8 K, observed in the dc measurements is present in the ac measurements and is more pronounced for higher frequencies. Below 4 K, the $\chi' T$ curves for the different frequencies start to diverge and a concomitant frequency dependent χ'' signal is observed. At the 1.8 K limit of our magnetometer, no peaks in χ'' are seen. However, the magnitude of the out-of phase signal, χ'' is around 40% of the in-phase signal, χ' at 1.8 K (ν = 10 kHz) consistent with the slow magnetic relaxation observed in SMMs.

To verify that **1** is a SMM, magnetisation *vs.* applied field hysteresis loops were obtained on single crystals of **1** using a micro-SQUID and are shown in Fig. 5, with the field oriented parallel to the easy axis of magnetization of the crystal.[11] The loops show magnetic hysteresis, which is temperature and sweep rate dependent, and hence **1** is an SMM. For a well-isolated SMM the first step in the hysteresis loop due to quantum tunnelling should occur at zero field. For **1**, due to small intermolecular interactions, this step is shifted to ±30 mT, which suggests a very small antiferromagnetic exchange bias between molecules of about 30 mT (see Fig. 5(a)). A step at zero field is also seen, and **1** is better described as a weakly exchange-biased SMM with fast tunnelling at zero field. The coercive field is much smaller than observed for Mn-based SMMs, no doubt due to the very fast tunnelling in **1**.

Although monomeric copper(II) complexes with H_3L and H_2L^- are well known,[12] **1** contains the first structurally characterised

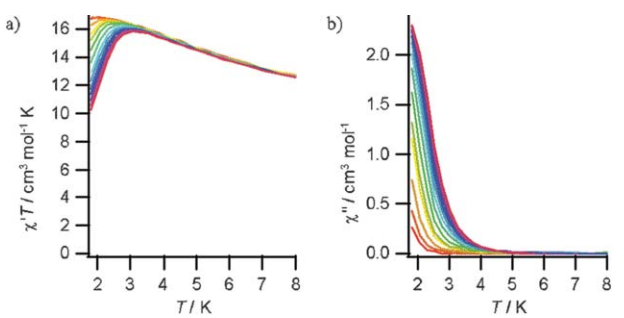

Fig. 4 Ac susceptibility for **1** measured in zero dc field {ν = 130 Hz (red) to 10 kHz (violet)} and plotted as (a) $\chi' T$ *vs.* T and (b) χ'' *vs.* T.

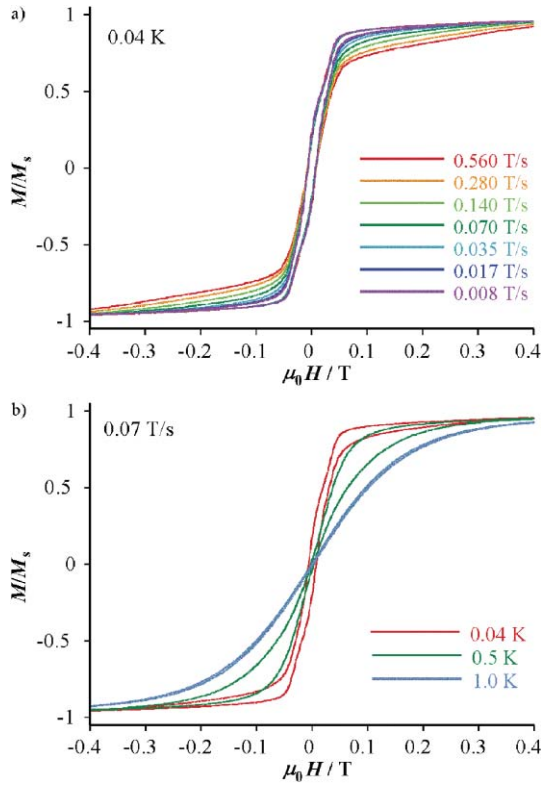

Fig. 5 Magnetisation (M) *vs.* applied dc field (H) hysteresis loops for a single crystal of **1** at the indicated field sweep rates (a) and temperatures (b). The magnetisation is normalised to the saturation value (M_s).

cobalt complex with this ligand. In fact, the coordination chemistry of this ligand with the first row transition-metal ions has been limited to copper(II) and nickel(II).[13] The Co_7 core of **1** is similar to that seen in other heptanuclear cobalt complexes, such as $[Co^{III}Co^{II}_6(thme)_2(O_2CCMe_3)_8Br_2]^-$ **2**,[14] $[Co^{II}_7(bzp)_6(N_3)_9(CH_3O)_3]$ **3**,[3c] and a fragment of a 1D polymer $[Co_8(H_2O)_2(OAc)_7(ampd)_6]_n$ **4**.[15] In ac susceptibility measurements, both **2** and **4** show no χ'' signals down to 1.8 K. **3** shows the onset of small (χ'' about 10% the size of χ' at comparable frequencies to our measurements) frequency dependent χ'' signals and no hysteresis down to 40 mK. So, despite **3** having a larger effective spin, $S' = 7/2$, a comparison of the ac data shows that **1** ($S' = 2$) has a larger effective energy barrier. The heptanuclear complexes **2** and **3** have C_i point symmetry, and the heptanuclear fragment in **4** has C_2 symmetry. The point symmetry of the Co_7 complex found in **1** is C_3 and hence the rhombic anisotropy (E) will be zero.[16] The absence of an E term, which mixes sublevels and leads to fast relaxation of the magnetisation in SMMs is a key property of this Co_7 complex. This allows us to observe slow magnetic relaxation in the form of strong frequency dependent χ'' signals in zero dc field and more importantly, temperature and sweep rate dependent hysteresis loops below 1 K. Ac susceptibility measurements to lower temperatures, to determine the energy barrier to reorientation of the magnetisation, will be carried out and reported in a full paper. Future work will focus on the preparation of mixed-metal analogues to replace the diamagnetic Co(III) and on ligand design to separate the Co_7 clusters in the crystal lattice. This will provide both further analogues for magnetic studies and a method of tuning the small intermolecular interactions.

We thank the University of Glasgow and EPSRC for financial support.

Notes and references

‡ Air-dried crystals analyse as **1**·MeOH·4H_2O, analysis (%) calc. (found) for $C_{25}H_{72}Co_7N_{11}O_{41}$: C, 18.82 (18.65); H, 4.55 (4.24); N, 9.65 (9.41). Selected IR data in cm^{-1}: 3230s, 2874m, 1592w, 1304vs, 1057s, 1007vs, 816s, 683s, 617vs. Intensity data were collected using a Bruker APEX2 CCD diffractometer equipped with graphite-monochromated Mo-Kα radiation (λ = 0.71073 Å) and an Oxford Cryosystems low-temperature device. The structure was solved by direct methods using SIR92 and refined using full-matrix least-squares refinement on F^2 using CRYSTALS. Non-hydrogen atoms were refined anisotropically; all hydrogen atoms were placed geometrically and refined as riding groups. The hydrogen atom bound to O14 was constrained to be 50% disordered over two sites. 367 electrons per unit cell were modelled as two disordered nitrate anions, 12 disordered solvent methanol and nine disordered solvent water molecules per unit cell using the BYPASS method of van der Sluis and Spek implemented within PLATON. *Crystal data* for **1**·9MeOH·4.5H_2O: trigonal, $P\bar{3}$, a = 19.3410(3), c = 11.5145(4) Å, U = 3730.21(15) $Å^3$, M = 1860.8, Z = 2, μ(Mo-Kα) = 1.627, T = 100 K; refinement used 242 parameters and gave $R1$ = 0.0343 for 3411 data with $F_o > 4\sigma(F)$, $wR2$ = 0.0526 for 5120 unique data ($2\theta \leqslant 27°$) and 0 restraints. CCDC 639649. For crystallographic data in CIF or other electronic format see DOI: 10.1039/b706238a. Dc magnetic measurements were carried out on air-dried samples (**1**·MeOH·4H_2O) using a Quantum Design MPMS-XL SQUID magnetometer, with the sample restrained between the two halves of an inverted gelatine capsule. A diamagnetic correction of 798 × 10^{-6} cm^3 mol^{-1} has been applied to the dc susceptibility data. Ac measurements were carried out using a Quantum Design PPMS magnetometer, with air-dried samples restrained in eicosane (zero dc field, 3 G ac drive field and ν = 130, 225, 476, 976, 1267, 1997, 2997, 3997, …, 9997 Hz). Hysteresis loops were collected on a single crystal of **1**·9MeOH·4.5H_2O using a micro-SQUID with the field applied along the easy axis of magnetization of the crystal.

1 A. Mishra, W. Wernsdorfer, S. Parsons, G. Christou and E. K. Brechin, *Chem. Commun.*, 2005, 2086.
2 E. C. Yang, D. N. Hendrickson, W. Wernsdorfer, M. Nakano, L. N. Zakharov, R. D. Sommer, A. L. Rheingold, M. Ledezma-Gairaud and G. Christou, *J. Appl. Phys.*, 2002, **91**, 7382.
3 (*a*) M. Murrie, S. J. Teat, H. Stœckli-Evans and H. U. Güdel, *Angew. Chem., Int. Ed.*, 2003, **42**, 4653; (*b*) S. J. Langley, M. Helliwell, R. Sessoli, P. Rosa, W. Wernsdorfer and R. E. P. Winpenny, *Chem. Commun.*, 2005, **40**, 5029; (*c*) Y.-Z. Zhang, W. Wernsdorfer, F. Pan, Z.-M. Wang and S. Gao, *Chem. Commun.*, 2006, 3302; (*d*) M.-H. Zeng, M.-X. Yao, H. Liang, W.-X. Zhang and X.-M. Chen, *Angew. Chem., Int. Ed.*, 2007, **46**, 1832.
4 A. Ferguson, A. Parkin and M. Murrie, *Dalton Trans.*, 2006, 3627.
5 A. Ferguson, K. Thomson, A. Parkin, P. Cooper, C. J. Milios, E. K. Brechin and M. Murrie, *Dalton Trans.*, 2007, 728.
6 W. Liu and H. H. Thorp, *Inorg. Chem.*, 1993, **32**, 4102.
7 G. Aromí, H. Stoeckli-Evans, S. J. Teat, J. Cano and J. Ribas, *J. Mater. Chem.*, 2006, **16**, 2635; B. N. Figgis, M. Gerloch, J. Lewis, F. E. Mabbs and G. A. Webb, *J. Chem. Soc. A*, 1968, 2086.
8 E. K. Brechin, O. Cador, A. Caneschi, C. Cadiou, S. G. Harris, S. Parsons, M. Vonci and R. E. P. Winpenny, *Chem. Commun.*, 2002, 1860.
9 J. M. Clemente-Juan, E. Coronado, A. Forment-Aliaga, J. R. Galán-Mascarós, C. Giménez-Saiz and C. J. Gómez-García, *Inorg. Chem.*, 2004, **43**, 2689.
10 O. Kahn, *Molecular Magnetism*, VCH, Weinheim, 1993, p. 42.
11 W. Wernsdorfer, *Adv. Chem. Phys.*, 2001, **118**, 99.
12 G. J. M. Ivarsson, *Acta Crystallogr., Sect. C: Cryst. Struct. Commun.*, 1984, **40**, 67.
13 G. J. M. Ivarsson, *Acta Crystallogr., Sect. B: Struct. Crystallogr. Cryst. Chem.*, 1982, **38**, 1828.
14 M. Moragues-Canovás, C. E. Talbot-Eeckelaers, L. Catala, F. Lloret, W. Wernsdorfer, E. K. Brechin and T. Mallah, *Inorg. Chem.*, 2006, **45**, 7038.
15 K. G. Alley, R. Bircher, O. Waldmann, S. T. Ochsenbein, H. U. Gudel, B. Moubaraki, K. S. Murray, F. Fernandez-Alonso, B. F. Abrahams and C. Boskovic, *Inorg. Chem.*, 2006, **45**, 8950.
16 D. Gatteschi and L. Sorace, *J. Solid State Chem.*, 2001, **159**, 253.